Experimental and Numerical Assessment of Slat Cove Liners

Michael Pott-Pollenske[1], Meike Jansen[2] und Juergen Dierke[3]

DLR Institute of Aerodynamics and Flow Technology, 38108 Braunschweig

[1] *e-mail: michael.pott-pollenske@dlr.de*

[2] *e-mail: meike.jansen@dlr.de*

[3] *e-mail: juergen.dierke@dlr.de*

Introduction

High-lift-systems are a major contributor to the airframe noise foot print of a modern transport aircraft. The most crucial element is still the slat, which is first the dominant source of broadband noise and second enables the required aerodynamic performance at low approach and landing speeds. In the recent past several technologies were investigated showing a high potential to reduce slat noise but being unsuited for retro-fitting of existing aircraft. One promising noise reduction technology is a slat cover liner as was investigated in the German LuFo project MOVE.ON [1], [2] and later on studied in the EU co-funded research project InVentor [3].

The scope of InVentor in this context was to study different absorber materials, some of them manufactured by means of additive layer manufacturing, for the use in a slat cover liner. Apart from the material properties also the position and dimension of the cove liner were investigated. The tests were conducted in three wind tunnels, the AWT at the University of Bristol, ONERA's F2 wind tunnel and DLR's Acoustic Wind Tunnel in Braunschweig (AWB). In the course of the studies it turned out that mechanical integration issues like very small steps may introduce perturbations suited to generate excess noise, which adversely affects the achievable noise reduction.

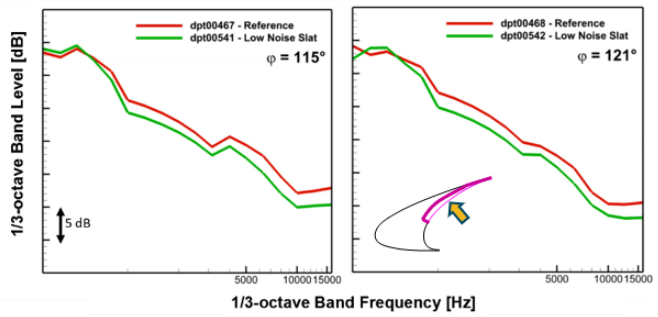

Figure 1: Noise reduction as achieved with a slat cove liner tested with the large scale DLR F15LS high-lift system (clean chord 1200 mm)

The achievable noise reduction is shown in Figure 1 in terms of 1/3-octave band spectra measured for slightly rear arc radiation directions in DNW-LLF. As is visible, the tests revealed a broadband 2 - 3 dB noise reduction.

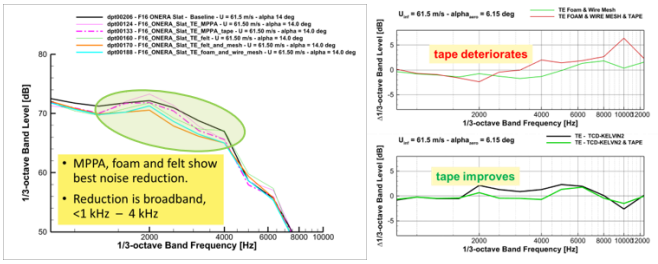

Figure 2: Noise reduction as achieved with a slat cove liner tested in InVentor with the small scale DLR F16 high-lift system. Left: summary of selected results. Right: effect of tape used to change the liner's dimensions (clean chord 300 mm)

The effects observed within InVentor are visualized in Figure 2. On the left hand side 1/3-octave band sound pressure level spectra are presented showing the acoustic effects of different liner configurations. On the right hand side the noise level differences for selected liners are displayed. Tape was applied in order to change the liner's streamwise extend for two samples in exactly the same manner, meaning tape position, type and thickness. As is visible the effects are contradicting meaning improving the noise reduction (lower graph) or deteriorating the noise benefit (upper graph).

Problem Statement

In order to mature the technology for an industrial use, uncertainties with respect to the liner's installation needs to be minimized. This can be achieved by clear manufacturing and installation guidelines or appropriate methods and tools. One problem by definition is that the formulation of guidelines requires very detailed knowledge about the product itself with most of the data being the OEM's intellectual property, which is typically not shared. The complexity of "tool application" is discussed in the following.

Figure 3 shows the backside of a real Airbus A320 outboard slat. It is clearly visible that the slat cove is not a smooth surface. Seals, slat tracks, slat links and other parts require space and come along with specific demands in terms of clearances, repair procedures and other constraints.

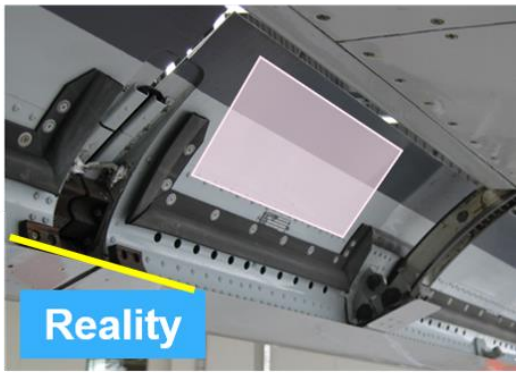

Figure 3: View into the slat cove of an outboard slat of the Airbus A320 aircraft. Potential area for a liner is highlighted by the light grey rectangle

Compared with this slat the model type slats as shown in Figure 4 look very clean. In large scale, by the way comparable in dimension to the Airbus A320 outboard slat, the liner extended over the entire back skin of the slat. Compared with the original type slat such configuration is not doable at all. The more realistic small scale liner might be integrated in a real slat but will be segmented in spanwise and chordwise direction.

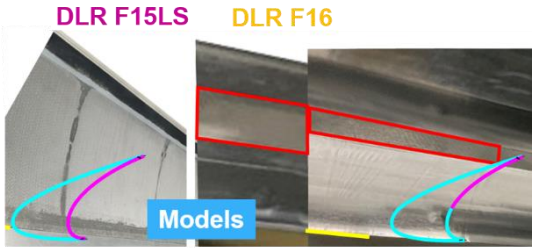

Figure 4: Large scale (left) and small scale (right) realization of slat cove liners. Liner extend is visualized by purple line in inserted sketch

For the design of a slat cove liner one can conclude three basic questions:

1. Which scale / dimension is representative and affordable?
2. Is it necessary to represent all technical details in the design phase?
3. How do we treat acoustic uncertainties and how do we judge on maturity?

With respect to point 1 and 2 a full scale and fully detailed mockup up, realized experimentally or numerically, represents the best case scenario. For plausible reasons like e.g. costs, it is unrealistic and compromises are required including possible implications on the meaningfulness of the mock-up. Topic 3 will be addressed in the remainder of this work.

Component Noise Prediction

Typically, the semi-empirical component noise prediction does not consider neither special installation constraints of a device on the aircraft nor the integration of a noise reduction technology (NRT) on a particular device. Moreover, the noise reduction is actually only accounted for with the simple addition of sound pressure level differences, either in terms of overall sound pressure levels or in terms of spectral representations.

What is now proposed on example of the slat cover liner is the coupling of the semi-empirical noise prediction, e.g. with the DLR PROFAN suite, with cheap and fast numerical fluid dynamics and computational aeroacoustics tools.

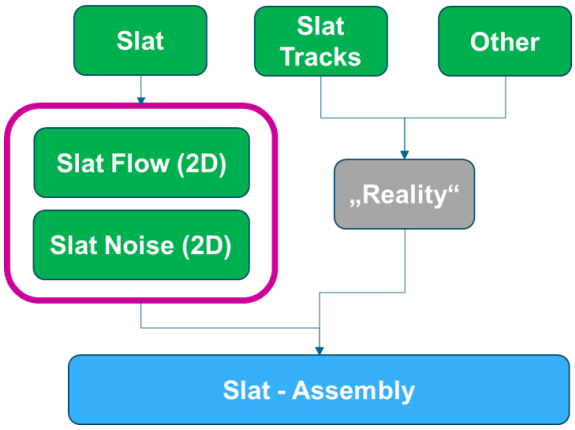

Figure 5: Slat noise prediction for the slat cover liner including numerically determined acoustic installation uncertainties

The block diagram (Figure 5) shows the procedure, which consists from top to bottom of the semi-empirical slat noise prediction, followed by the numerical branch devoted to the evaluation of the NRT's installation. In parallel slat track noise and, if feasible, other stuff is evaluated. In the current context such sources are considered "as is" and therefore summarized as constants under "Reality". Finally, all components will be added to the total slat assembly's noise generation.

Flow and Noise Simulation

The basis for the simulation tool chain is a fast and accurate 2-dimensional RANS based flow simulation, which is carried out by means of the DLR flow solver FLOWer [4]. As demonstrated in studies with small and large scale wind tunnel models [5], the transposition form 2D to 3D is quite straight forward, which justifies the use of a 2D CFD method. The DLR CAA solver DISCO [6] was applied to evaluate and quantify acoustic effects.

2D RANS Flow Simulation

The application of tape, potentially causing miniature type bumps or steps, was simulated in the flow simulations. Bumps were generated at 9 positions in the slat cove which were all located downstream of the stagnation point. The simulations were carried out individually for each bump. Figure 6 visualizes the entire flowfield showing the velocity in terms of Ma-number contours and streamlines. The turbulent kinetic energy is represented as difference between the reference configuration without bumps and the bump configurations. Please note, that only two bump positions are

display in Figure 6 in order to highlight the separate TKE maxima generated at each bump.

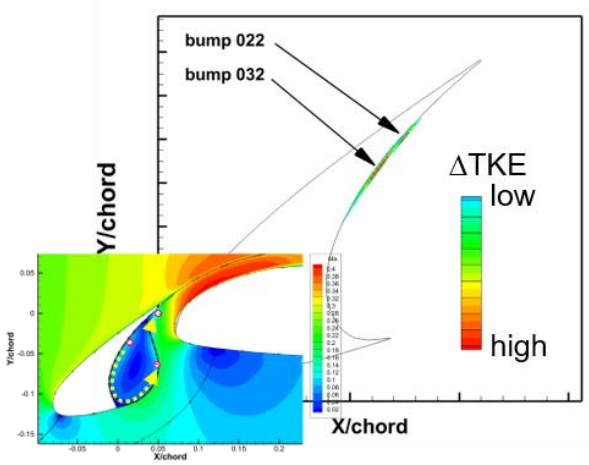

Figure 6: Representation of the slat flowfield (lower left) and the exemplary presentation of TKE spots in the slat cove generated by shape discontinuities

A key question is, if the relative maxima of the TKE already represents an acoustic quantity which can be evaluated and would consequently let the CAA simulations appear obsolete. However, this question might be finally answered at another point in time. For the present work the turbulence generation as such is considered important, because the turbulence is convected with the flowfield and thereby eddies are accelerated and distorted, which in summary is suited to generate noise. This is verified in the next step by means of the DISCO computations.

2D Acoustic Simulations

The DLR DISCO CAA solver is a discontinous Galerkin code, which was tested and validated for use with high lift systems. Unsteady turbulent sound sources are modeled by means of stochastic sources based on Ewert's RPM model. [8]. As is visible in Figure 7 and Figure 8 the aforementioned relative TKE maxima are visible in the TKE contour plots. Figure 7 provides the comparison between the Reference configuration and the bump at position 22.

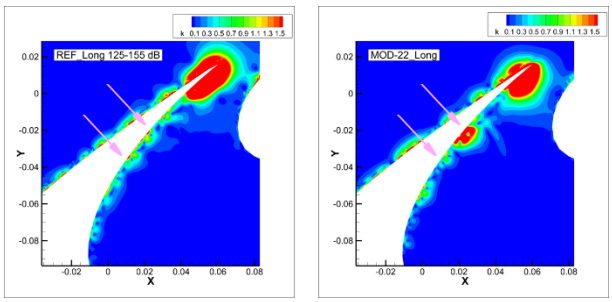

Figure 7: TKE representation as computed by the CAA solver DISCO on basis of the RPM method.
Left: Reference
Right: Bump at pos 22 causing relative TKE maximum

In Figure 8 the bump is located at the slightly downstream located position 27. It should be emphasized that for the bump at pos 27 an TKE maxima at pos. 22 vanished completely while the new TKE spot emerged.

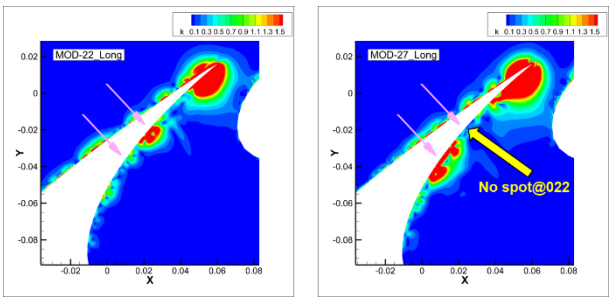

Figure 8: TKE representation as computed by the CAA solver DISCO on basis of the RPM method.
Left: Bump at pos 22 causing relative TKE maximum
Right: Bump at pos 27 causing separate relative TKE maximum

The final acoustic evaluation was first carried out by the analysis of 1/3-octave band sound pressure level spectra. This analysis revealed sound pressure level maxima in the frequency range between 1600 Hz and 3150 Hz for polar radiation directions of $60° < \varphi_x < 150°$. In the following the directivity patterns for two representative 1/3-octave band frequencies out of the bandwidth of maximum levels are presented.

Figure 9 shows the directivity pattern for the 1600 Hz 1/3-octave band. The reference is represented by red curves while bump 22 and bump 27 are represented with green and blue curves. As is visible, differences between the reference and the modifications are small. In case of the frequency of 1600 Hz the bump 22 exceeds slightly the reference.

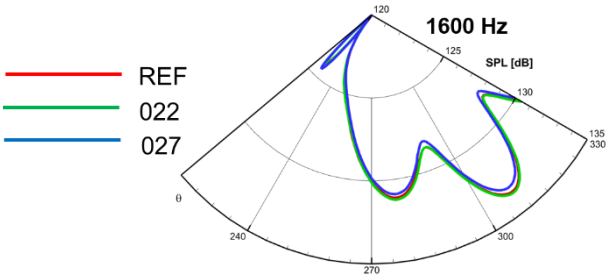

Figure 9: Directivity patterns as simulated for the 1600Hz 1/3-octave band frequency.
Red: Reference / Green: bump at pos. 22 / Blue: bump at pos. 27

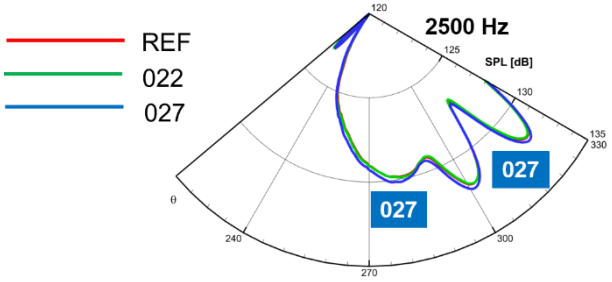

Figure 10: Directivity patterns as simulated for the 2500Hz 1/3-octave band frequency. Red: Reference / Green: bump at pos. 22 / Blue: bump at pos. 27

For the higher 1/3-octave band of 2500 Hz the bump at pos. 27 seems to finally generate the highest noise levels (Figure 10) but again the differences are very small compared to the experimental data.

Summary and Conclusion

In the current work it was tested if numerical tools can be applied to assess the robustness and maturity of a noise reduction concept with respect to its installation and integration into a high-lift device. The procedure was exemplified for a slat cove liner.

The selected 2D simulation tools would afford about one day computational time for a full dataset, which seems to fit into industrial needs.

The results are currently twofold. On the positive side it can be noted that, in principle, the computational data follow the experimental results. But, and this is the negative aspect, the magnitudes of the obtained noise level changes are quite small when compared to the experimental results.

These findings lead to questions.

1. Are the results a lucky coincidence?
2. If not, what physical or computational reasons led to such small sound pressure level differences?
3. Are the applied tools and methods suitable for the scope?

A full set of answers is not available at this point in time. But some ideas exist, which are formulated as workplan in the outlook

Outlook

The authors do not believe in a lucky coincidence. Up to now there is no evidence pointing in this direction.

It seems reasonable to check the CAA tool in the following respects.

First, the stochastic modelling of turbulent sound sources and thus the adequate application of the (F)RPM method is based on best practices to compute major airframe noise sources. It might be the case that the sources we wanted to resolve in the present study are not represented or better say modeled by the applied best practice methods. This needs to be assessed.

Second, the convection of eddies over sufficiently long distances might not be ensured by the computational grid. A second set of computations with refined grid(s) is envisaged in order to prove or to discard this option.

For the near future we will continue the investigation for the slat cove liner.

Literature

[1] Gölling, B. & Airbus Operations GmbH (2016): "Multi-Optimierung und Verifizierung von Entwürfen durch PerfOrmaNce Tests und Simulationen: MOVable dEsign, Optimisation and airframe Noise reduction", LuFo IV-4 Förderprojekt des BMWi der Bundesregierung, Schlussbericht

[2] Pott-Pollenske, M.: "Development of a Slat Cover Liner", AIAA AVIATION 2021 FORUM, August 2-6, 2021, Virtual event, https://doi.org/10.2514/6.2021-2114

[3] Manoha, E.: "INVENTOR: A Collaborative European Initiative Driving Innovation in Airframe Noise Reduction", 14th European Aeronautics Science Network (EASN) International Conference, Edition October 8 – 11, 2024

[4] Wild, J.: "Validation of Numerical Optimization of High-Lift Multi-Element Airfoils based on Navier-Stokes-Equations", AIAA Paper 2002-2939, 20th AIAA Applied Aerodynamics Conference, June 24-26, 2002, St. Louis, Missouri, USA

[5] Pott-Pollenske, M., Delfs, J., Reichenberger, J.: "A Testbed for large scale and high Reynolds number Airframe Noise Research", 19th AIAA/CEAS Aeroacoustics Conference, May 27-29, 2013, Berlin, Germany, https://doi.org/10.2514/6.2013-2260

[6] Bauer, M.: "Airframe noise prediction using a discontinuous Galerkin method.", DLR-Forschungsbericht. DLR-FB 2011-11, Dissertation, Institut für Aerodynamik und Strömungstechnik, 121 S, 2011

[7] Ewert, R., Dierke, J., Neifeld, A., Appel, C., Siefert, M., Kornow, O.: "CAA broadband noise prediction for aeroacoustic design", Procedia Engineering, Volume 6, 2010, Pages 254-263, ISSN 1877-7058, https://doi.org/10.1016/j.proeng.2010.09.027. (https://www.sciencedirect.com/science/article/pii/S1877705810005734)

[8] Ewert, R.: "Broadband slat noise prediction based on CAA and stochastic sound sources from a fast random particle-mesh (RPM) method", Computers & Fluids Vol. 37, pages 369 – 387, Pergamon 2008/5/1